Journal of Neuroendocrinology
From Molecular to Translational Neurobiology

Journal of Neuroendocrinology **23**, 1204–1213

ORIGINAL ARTICLE

Transient Receptor Potential Channel M4 and M5 in Magnocellular Cells in Rat Supraoptic and Paraventricular Nuclei

R. Teruyama*, M. Sakuraba†, H. Kurotaki* and W. E. Armstrong†

**Department of Biological Sciences, Louisiana State University, LA, USA.*

†Department of Anatomy and Neurobiology, University of Tennessee, Baton Rouge, Health Science Center, Memphis, TN, USA.

Journal of Neuroendocrinology

The neurohypophysial hormones, vasopressin (VP) and oxytocin (OT), are synthesised by magnocellular cells in the supraoptic nucleus (SON) and the paraventricular nucleus (PVN) of the hypothalamus. The release of VP into the general circulation from the neurohypophysis increases during hyperosmolality, hypotension and hypovolaemia. VP neurones increase hormone release by increasing their firing rate as a result of adopting a phasic bursting. Depolarising after potentials (DAPs) following a series of action potentials are considered to be involved in the generation of the phasic bursts by summating to plateau potentials. We recently discovered a fast DAP (fDAP) in addition to the slower DAP characterised previously. Almost all VP neurones expressed the fDAP, whereas only 16% of OT neurones had this property, which implicates the involvement of fDAP in the generation of the firing patterns in VP neurones. Our findings obtained from electrophysiological experiments suggested that the ionic current underlying the fDAP is mediated by those of two closely-related Ca^{2+}-activated cation channels: the melastatin-related subfamily of transient receptor potential channels, TRPM4 and TRPM5. In the present study, double/triple immunofluorescence microscopy and reverse transcriptase-polymerase chain reaction techniques were employed to evaluate whether TRPM4 and TRPM5 are specifically located in VP neurones. Using specific antibodies against these channels, TRPM5 immunoreactivity was found almost exclusively in VP neurones, but not in OT neurones in both the SON and PVN. The most prominent TRPM5 immunoreactivity was in the dendrites of VP neurones. By contrast, most TRPM4 immunoreactivity occurred in cell bodies of both VP and OT neurones. TRPM4 and TRPM5 mRNA were both found in a cDNA library derived from SON punches. These results indictate the possible involvement of TRPM5 in the generation of the fDAP, and these channels may play an important role in determining the distinct firing properties of VP neurones in the SON.

Key words: fast depolarsing after potential, vasopressin, oxytocin.

doi: 10.1111/j.1365-2826.2011.02211.x

Correspondence to:
R. Teruyama, Department of Biological Sciences, Louisiana State University, 202 Life Sciences Building, Baton Rouge, LA 70803, USA (e-mail: rteruyama@lsu.edu).

The neurohypophysial hormones, vasopressin (VP) and oxytocin (OT), are synthesised by the magnocellular cells (MNCs) in the paraventricular nucleus (PVN), supraoptic (SON) and accessory nuclei of the hypothalamus. These hormones are released into the general circulation from the neurohypophysis in response to physiological demands. The release of VP is induced by hyperosmolality (1), hypovolaemia (2) and hypotension (3), and exerts both antidiuretic and pressor effects. The release of VP is precisely regulated by the rate and pattern of firing activity in MNCs (4, 5). VP neurones implement a phasic firing pattern consisting of alternating periods of activity and silence, each lasting tens of seconds, during the demand for VP. This pattern maximises hormone release through the facilitation and the avoidance of secretory fatigue (4, 6).

The firing pattern of VP neurones is critically regulated by intrinsic membrane properties, especially depolarising afterpotentials (DAPs). The summation of DAPs induces a plateau potential that underlies the burst of action potentials in phasic neurones (7, 8). We demonstrated, in VP neurones, that DAPs can be divided into the classically observed slow DAP (approximately 2 s) (7, 9), and a Ca^{2+}-activated nonselective cation (CAN) current that underlies a

fast DAP (fDAP) (approximately 200 ms) (10). Interestingly, immunoidentification of recorded neurones revealed that almost all VP neurones, but only 16% of OT neurones, expressed the fDAP, implicating the involvement of fDAP in the generation of the specific firing patterns observed in VP neurones (10). Currently, the superfamily of transient receptor potential (TRP) channels are the only molecularly identified CAN channels. Of the 26 identified mammalian TRP channels, two of the melastatin-related subfamily, TRPM4 and TRPM5, share some of the hallmarks of the CAN current responsible for the generation of the fDAP in VP neurones. Both TRPM4 and TRPM5 include Ca^{2+} activation, selectivity for monovalent cations, voltage-dependency and sensitivity to the nonsteroidal anti-inflammatory drug, flufenamic acid (11–15). These two TRP channels therefore represent good candidates for the mechanism underlying the fDAP in VP neurones. The present study was conducted to determine whether TRPM4 and/or TRPM5 are specifically located in VP neurones using reverse transcriptase-polymerase chain reaction (RT-PCR) and immunocytochemical techniques.

Materials and methods

Animals

Male and female adult Sprague-Dawley rats were used (180–210 g body weight; Harlan Laboratories, Indianapolis, IN, USA). The rats were housed in a room under a 12 : 12 h light/dark cycle with access to food and water available *ad lib.* All protocols were approved by the Institutional Animal Care and Use Committee at the Louisiana State University and the University of Tennessee.

Immunocytochemistry

The rats were deeply anaesthetised with sodium pentobarbital (50 mg/kg, i.p.) and perfused through the heart with 0.01 M sodium phosphate-buffered saline (pH 7.2–7.4), followed by a fixative of 4% paraformaldehyde in 0.1 M sodium phosphate buffer (pH 7.2–7.4). The brains were excised and post-fixed in the same fixative for 1–3 days, then sectioned at 40 μm on a vibrating microtome (VT1000; Leica, Bannockburn, IL, USA). To produce polyclonal antibodies against TRPM4, a 15-amino acid synthetic peptide corresponding to amino acids 60–74 (NH2-TEWNSDEHTTEKPTDC-COOH) of the amino-terminal tail of the rat TRPM4 with an added carboxyl-terminal cysteine was synthesised (AnaSpec, Fremont, CA, USA). The sequences were chosen using the antibody design software NHLBIAB-DESIGNER (under development; NIH, Bethesda, MD, USA) for specificity, and the absence of likely post-translational modifications using computer analysis. The carboxyl-terminal cysteine was used to conjugate the peptide to keyhole limpet haemocyanin carrier protein for immunisation. The peptide was used for immunisation of rabbits using a standard immunisation protocol (Covance, Denver, PA, USA). The antisera (LS102) employed in the present study was affinity-purified on a column made with the same synthetic peptide used for the immunisations (SulfoLink Antibody Immobilization kits; Pierce, Rockford, IL, USA).

Polyclonal antibody against TRPM5 (N-20) was raised in goat (Santa Cruz Biotechnology, Santa Cruz, CA, USA). These TRPM4 and TRPM5 antibodies were used in free-floating brain slices for 48–72 h at 4 °C at dilutions of 1 : 2500 for 1 : 500, respectively. For single staining of TRPM4 and TRPM5, the brain slices were subsequently incubated with biotinylated goat anti-rabbit and rabbit anti-goat secondary antibodies (dilution 1 : 200), respectively, followed by the standard ABC-diaminobenzidine procedure per the protocol provided by Vector (Burlingame, CA, USA). The brain sections were mounted on gelatin-coated slides, dehydrated, cleared and cover slipped with Permount. Light microscopic images were acquired digitally IP LAB software (Scananalytics, Fairfax, VA, USA) and a cooled charge-coupled device camera (Photometrics SenSys Cam, Tucson, AZ, USA). Digital images were minimally adjusted in ADOBE PHOTOSHOP (Adobe Systems Inc., San Jose, CA, USA) with small changes in dynamic range. Absorption controls for TRPM4 and TRPM5 antibodies were run with 20 and 40 μg, respectively, of control peptide per 1 ml of antibody at the dilution used for staining.

For double immunofluorescence, following incubation with TRPM4 antibody, the brain slices were further incubated with either OT-neurophysin (NP) or VP-NP mouse monoclonal antibodies (PS38 and PS41, respectively: provided by H. Gainer, NIH) used at a dilution of 1 : 500. For triple immunofluorescence, following incubation with TRPM5 antibody, the brain slices were further incubated with a cocktail containing OT-NP (PS38) antibody at a dilution of 1 : 500 and polyclonal rabbit VP-NP antiserum at a dilution of 1 : 20 000 provided by Alan Robinson (UCLA, Los Angeles, CA). The OT- and VP-NP antisera are well characterised (16), and therefore we did not conduct absorption tests. All antibodies and other labelling reagents were dissolved in phosphate-buffered saline (PBS) containing 0.5% Triton X-100. Following the incubations with the primary antibodies, the sections were incubated in a cocktail of appropriate secondary antibodies conjugated with fluorescence markers (Invitrogen, Carlsbad, CA, USA) for 2–4 h at room temperature. The secondary antibodies used were: Alexa Fluor 568 conjugated goat anti-rabbit and Alexa Fluor 488 conjugated goat anti-mouse for double immunofluorescence; and Alexa Fluor 647 conjugated chicken anti-goat, Alexa Fluor 594 conjugated chicken anti-rabbit, and Alexa Fluor 488 conjugated chicken anti-mouse for triple immunofluorescence labelling. The sections were mounted in 50% glycerol in PBS or polyvinyl alcohol (PVA) with anti-fading agent 1,4-diazabicyclo[2.2.2]octane (DABCO) that consists of 4.8 g PVA, 12 g glycerol, 12 ml dH_20, 24 ml 0.2 M Tris-HCl and 1.25 g DABCO. TRPM4 immunoreactivity was visualised with either VP-NP or OT-NP immunoreactivity (double-staining), whereas that of TRPM5 was visualised with VP and OT immunoreactivities (triple-staining). Images were acquired with confocal microscopes (model #1024; Bio-Rad, Hercules, CA, USA; TCS SP2 spectral confocal microscope; Leica, Mannheim, Germany). Optical section thickness was 2 μm. These were viewed in stacks of three to five sections using IMAGEJ software (NIH).

RT-PCR

Tissue preparation

The rats were deeply anaesthetised with sodium pentobarbital (50 mg/kg, i.p.) and perfused through the heart with an artificial cerebral spinal fluid (aCSF) solution containing (in mM): 124 NaCl, 3 KCl, 2.0 $CaCl_2$, 1.3 $MgCl_2$, 1.24 NaH_2PO_4, 25 $NaHCO_3$, 0.2 ascorbic acid and 10 D-glucose (pH 7.4). The brains were removed and sliced in the coronal plane at a thickness of 250 μm using a vibrating microtome (Leica VT1000; Leica) in ice-cold aCSF. The SON tissues were collected in RNA stabilisation reagent, RNAlater (Qiagen, Valencia, CA, USA), using a punch-tool (inner diameter 1.5 mm) and total RNA was purified using RNeasy (Qiagen).

Single-cell harvest for single-cell RT-PCR

The brains were sliced as described above. Small pieces of brain (approximately 2 × 2 mm) containing SON were dissected from the brain slices under a stereomicroscope. This tissue was incubated in oxygenated aCSF (35 °C) containing Protease Type XIV (1.2 mg/ml: Sigma Chemicals, St Louis, MO, USA) for 20–30 min, and washed in a solution consisting of (mM): 140 sodium isethionate, 2 KCl, 4 $MgCl_2$, 23 glucose, 15 HEPES, pH 7.3 (adjusted

with 1 M NaOH). The enzyme-treated tissue was triturated in sodium isethionate solution using three successively smaller fire-polished pipettes to release individual MNC cell bodies. The supernatant containing dissociated neurones was then transferred to a plastic Petri dish (Nunc, Rochester, NY, USA) on an inverted microscope stage and allowed to settle for approximately 5 min. A background flow of approximately 1 ml/min of HEPES-buffered saline solution (HBSS) was then established. HBSS consisted of (mM): 138 NaCl, 3 KCl, 1 $MgCl_2$, 2 $CaCl_2$, 10 HEPES, 20 dextrose, pH 7.3 (adjusted with 1N NaOH) and osmolarity = 300–305 mosM. Glass capillary tubes for pipettes (Corning 7052 capillary glass; Garner Glass, Claremont, CA, USA) were autoclaved to prevent RNAse contamination. Electrodes were pulled on a Sutter Instrument (Novato, CA, USA) Model P-87 Flaming/Brown Micropipette puller, fire-polished and filled with HBSS made with RNAse free water. Positive pressure was applied when the electrode approached a cell to minimise contamination (i.e. extracellular matrix, dead cells, RNAse, etc.). The electrode with an attached cell was lifted into a stream of aCSF for washing and the cell was sucked into the pipette. Following aspiration, the contents of the electrode were ejected into a chilled 0.5-μl pre-siliconised RT tube containing cellular mixture [1.9 μl of diethylpyrocarbonate (DEPC)-treated water, 1.0 μl dNTPs (10 mM), 0.7 μl bovine serum albumin (143 ng/μl), 0.7 μl oligo-dT (0.5 ug/μl), 0.7 μl Superase-In (40 U/μl)]. The mixture was either stored at −80 °C or used immediately for RT.

RT

The mixture was heated to 65 °C for 5 min and placed on ice for at least 1 min. Single-stranded cDNA was synthesised from the cellular mRNA after adding 16 μl RT Master Mix (6.0 μl DEPC-treated water, 2.0 μl 10× RT buffer, 4.0 μl $MgCl_2$ (25 mM), 2.0 μl dithiothreitol (0.1 M), 1.0 Ul Rnase Out, 1.0 μl Superscript III). This mixture was incubated at 42 °C for 50 min and terminated by heating to 70 °C for 15 min. To eliminate any remaining RNA from the reaction, 0.5 μl Rnase H (2 U/μl) was added and the solution was incubated at 37 °C for 20 min. The cDNA was either stored at −80 °C or used immediately for PCR.

Table 1. Primer sequence used.

Gene	Primer sequence	Amplicon size
TRPM4	Forward 5′-CCTGCAGGCCCAGGTAGAGA-3′ Reverse 5′-TTCAGCAGAGCGTCCATGAG-3′	267 bp
TRPM5	Forward 5′-'GGCCAATTGGAGAAGTTAACAG-3′ Reverse 5′-AGGTGACACCAACAATGAACAG-3′	379 bp
VP	Forward 5′-GACGGTGGATCTCGGACTGAA -3′ Reverse 5′-CGCCCCTAAAGGTATCATCACAAA -3′	463 bp
OT	Forward 5′-CCTCACCTCTGCCTGCTACTT -3′ Reverse 5′-GGGGGCGATGGCTCAGTAGAC -3′	440 bp

PCR

The single-cell cDNA generated from the RT step was subjected to conventional PCR using a programmable thermal cycler from MJ Research (Waltham, MA, USA) and primers specifically designed to amplify the cDNA of interest (Table 1). Identification of each cDNA species is based on the predicted size of each PCR product. These experiments the determination of whther TRPM4 or TRPM5 were expressed by individual neurones. Negative controls for contamination from extraneous and genomic DNA from other sources were run for every batch of neurones tested.

Results

Localisation of TRPM4 immunoreactivity

At a dilution of 1 : 2000–5000, the TRPM4 antibody gave consistent results in several animals (seven males and one female). Within the sections containing the SON and the PVN, prominent immunoreactivity was observed in these nuclei and accessory neurosecretory nuclei, including the nucleus circularis and neurones within the medial forebrain bundle in the lateral hypothalamus. The immunoreactivity was densest in cell bodies of MNCs in the SON (Fig. 1A) and the PVN. Incubation of the antibody with the control peptide (20 μg/ml) used to generate this antibody completely eliminated specific immunoreactivity in the SON (Fig. 1) and the PVN, confirming the specificity of the antibody for the immunogen designed for detection of TRPM4.

Double fluorescence immunocytochemistry of TRPM4 and VP-NP/OT-NP using confocal microscopy was employed to elucidate whether TRPM4 was selectively located in VP or OT neurones. TRPM4 immunoreactivity was observed in most MNC cell bodies within the SON (Fig. 2A) and was seen in a cluster of cell bodies located in the lateral part of the PVN (Fig. 3A). Superimposed images in the SON (Fig. 2C) and PVN (Fig. 3C) demonstrated that

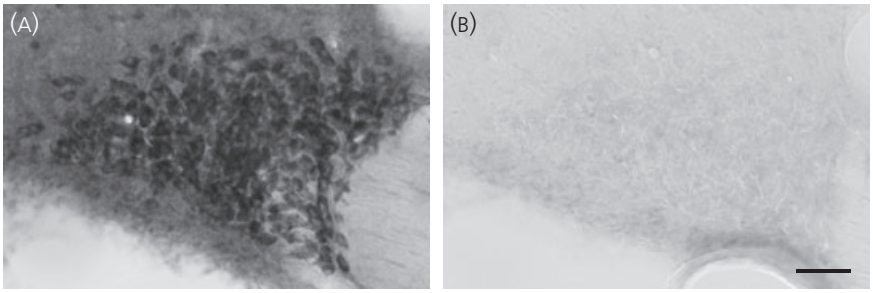

Fig. 1. Immunocytochemical localisation of TRPM4 in the supraoptic nucleus (SON). Immunocytochemistry of TRPM4 staining in the SON using the ABC method with antibody dilution of 1 : 2500 in 40-μm coronal sections. (A) Localisation of TRPM4 immunoreactivity in the rat SON. Immunoreactivity was found in the cell bodies of magnocellular cells. (B) Absorption control in the adjacent section to that in (A) using the same antibody dilution. Almost all immunoreactivity was abolished when 20 μg of control peptide was added to 1 ml of antibody solution, confirming the specificity of the antibody to the immunogen designed to detect TRPM4. Scale bars = 50 μm.

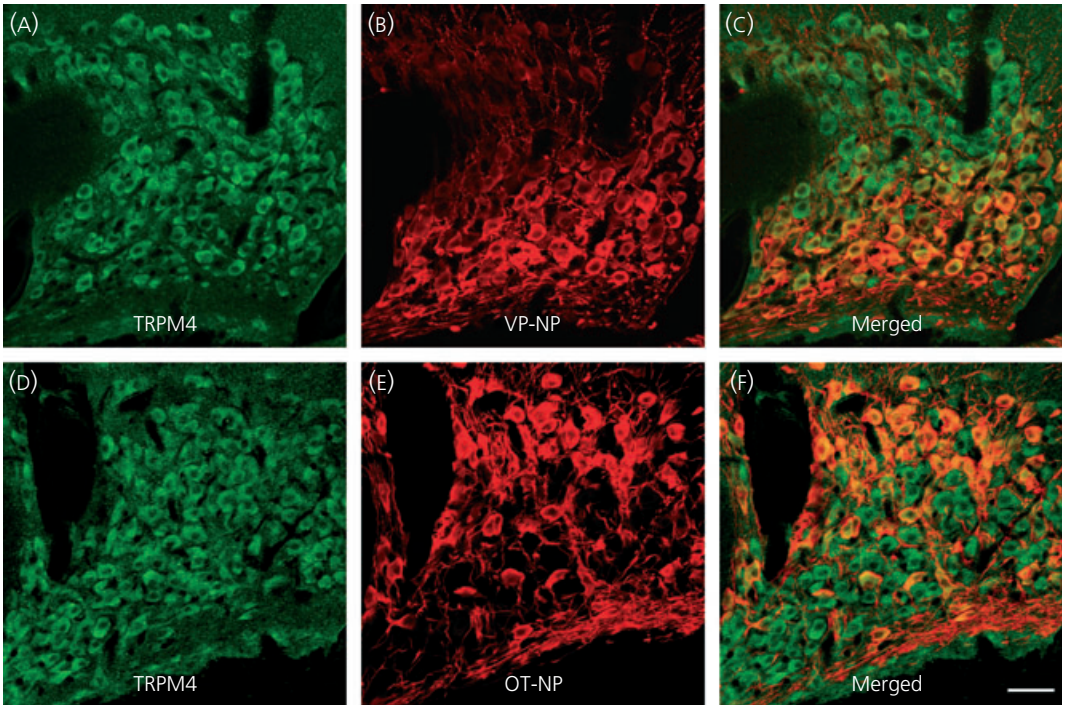

Fig. 2. Confocal double immunofluorescence of TRPM4 with vasopressin (VP)-neurophysin (NP) or oxytocin (OT)-NP in the supraoptic nucleus (SON). (A, D) Confocal photomicrographs of TRPM4 immunoreactivity labelled with Alexa Fluor 568-conjugated secondary antibody in the SON. TRPM4 immunoreactivity was observed in most of magnocellular cell bodies in the SON. (B) VP-NP immunoreactivity labelled with Alexa Fluor 488-conjugated secondary antibody in the same optical section as in (A). (C) Merged image of (A) and (B). The TRPM4 immunoreactivity was co-localised with VP-NP immunoreactivity as indicated by yellow produced by an overlap of the Alexa Fluor 568 and 488 labelled elements (arrows). (E) Confocal photomicrographs of OT-NP immunoreactivity labelled with Alexa Fluor 488-conjugated secondary antibody in the same section and image plane as in (D). (F) Merged image of (D) and (E). The TRPM4 immunoreactivity was also co-localised with OT-NP within the cell bodies in the SON. Scale bar = 50 μm.

the TRPM4 immunoreactivity was co-localised with both VP-NP and OT-NP immunoreactivities both in the SON and the PVN.

Localisation of TRPM5 immunoreactivity

At a dilution of 1 : 500, the TRPM5 antibody gave consistent results in all animals tested (eleven males and six females). Intense immunoreactivity was found in the sparsely located thick dendritic processes within the SON (Fig. 4A) and the PVN (Fig. 4B). Some dense immunoreactivity was also seen in several cell bodies within the SON (Fig. 4A), the PVN (Fig. 4B), the nucleus circularis and other accessory neurosecretory neurones within the medial forebrain bundle in the lateral hypothalamus. Absorption controls in adjacent sections from the same brain (50 μg/ml of control peptide) demonstrated that immunoreactivity was abolished (Fig. 4C), confirming the specificity of the antibody to the immunogen designed for TRPM5 detection.

Because the TRPM5 antibody was generated in goat, we could use triple-labelling fluorescence immunocytochemistry of TRPM5, VP-NP and OT-NP to determine whether TRPM5 was selectively located in VP or OT neurones. TRPM5, VP-NP and OT-NP immunoreactivities were labelled with Alexa Fluor 647, 594 and 488-conjugated secondary antibody, respectively, in the SON (Fig. 5) and the PVN (Fig. 6). In the SON, the most intense TRPM5 immunoreactivity was observed in the thick dendritic processes, whereas less intense, but still prominent TRPM5 immunoreactivity, was observed in the cell bodies (Fig. 5A). TRPM5 immunoreactivity was almost exclusively co-localised with VP-NP, but not OT-NP (Fig. 5A–D). Note that there is no co-localisation of TRPM5 solely with OT-NP immunoreactivity either in the processes or cell bodies. In rare cases, co-localisation of VP-NP and OT-NP immunoreactivites was observed, as shown in Fig. 5(D) (arrowheads). Those few OT-NP immunoreactive cells exhibiting TRPM5 contained VP-NP immunoreactivity, as indicated by the yellow colour. As in the SON, the most intense TRPM5 immunoreactivity was observed in the thick, dendritic-like processes in the PVN and was co-localised mostly with VP-NP, but not OT-NP (Fig. 6). The TRPM5 immunoreactive cells were also almost exclusively VP-NP immunoreactive in the PVN (Fig. 6). These findings were consistent in all animals tested (three male and four female rats).

RT-PCR detection of TRPM4 and TRPM5

We used RT-PCR to detect the presence of TRPM4 and TRPM5 in the SON. The SON (and immediately surrounding area) was punched from fresh brain slices and used to extract total RNA that was reverse transcribed. Rat kidney (13, 17, 18), heart (19) and tongue epithelial (20), tissues known to express TRPM4 and/or TRPM5 served as positive controls. The cDNA was amplified by PCR using

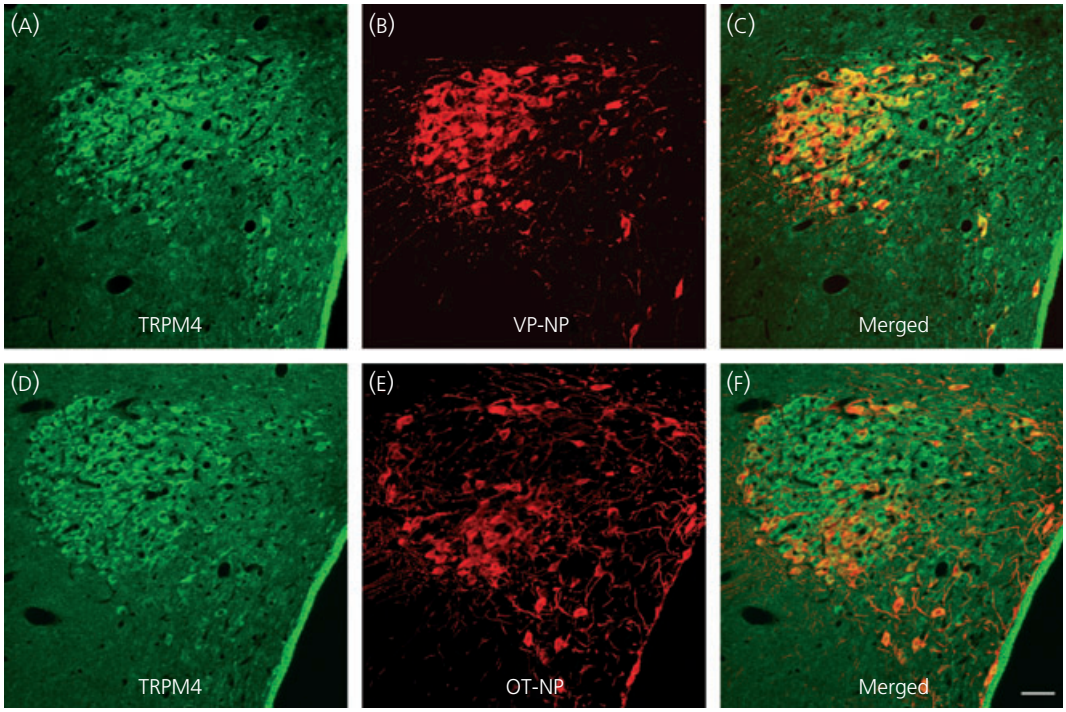

Fig. 3. Confocal double immunofluorescence of TRPM4 with vasopressin (VP)-neurophysin (NP) or oxytocin (OT)-NP in the paraventricular nucleus (PVN). (A) Confocal photomicrographs of TRPM4 immunoreactivity labelled with Alexa Fluor 568-conjugated secondary antibody in the PVN. Prominent TRPM4 immunoreactivity is observed in somata of magnocellular cells (MNCs) within the PVN. Most of these TRPM4 immunoreactive MNCs are located in a cluster of cells in the lateral magnocellular region; however, TRPM4 immunoreactive magnocellular cells are scattered in other regions of the PVN (dorsal, medial, ventrolateral and posterior parvocellular regions). There are no prominent TRPM4 immunoreactivities among parvocellular cells in the PVN. (B) VP-NP immunoreactivity labelled with Alexa Fluor 488-conjugated secondary antibody in the same 2-μm optical section as in (A). (C) Merged image of (A) and (B). The TRPM4 immunoreactivity was co-localised with VP-NP immunoreactivity, as indicated by yellow colour produced by an overlap of the Alexa Fluor 568 and 488 labelled elements. (D) Confocal photomicrographs of TRPM4 immunoreactivity taken in the same optical section as in (E). (E) OT-NP immunoreactivity labelled with Alexa Fluor 488-conjugated secondary antibody. (F) Merged image of (D) and (E). As in the supraoptic nucleus, TRPM4 immunoreactivity was also co-localised with OT-NP. Scale bar = 50 μm.

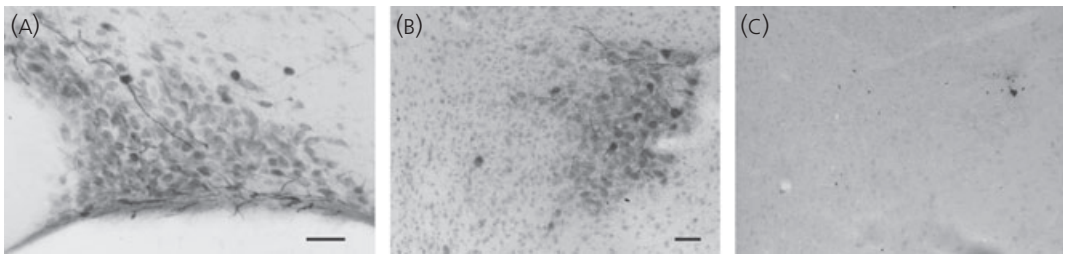

Fig. 4. Immunocytochemical localisation of TRPM5 in the supraoptic nucleus (SON) and the paraventricular nucleus (PVN). (A) Intense immunoreactivity for TRPM5 was found in a few thick dendritic processes within the SON. Some dense immunoreactivity was also seen in several cell bodies within the SON. (B) Intense immunoreactivity was found in the sparsely located thick dendritic processes within the PVN. Dense immunoreactivity was also seen in several cell bodies located in the lateral part of the PVN. (C) Absorption control in the section adjacent to that in (B), using the same antibody dilution. Immunoreactivity was completely abolished when 40 μg of control peptide was added to 1 ml of antibody solution. The standard ABC-diaminobenzidine method was used with antibody dilution of 1 : 500 in 40-μm coronal sections. Scale bar = 50 μm.

specific primers designed for TRPM4 and TRPM5. Amplified products were obtained at the expected sizes (266 bp for TRPM4 and 379 bp TRPM5) from the cDNA library derived from the SON tissue, as well as those from kidney, heart and tongue epithelial tissue (Fig. 7A,B).

To further test whether individual MNCs express TRPM4 and TRPM5, we performed single-cell RT-PCR. Individually dissociated MNCs were collected singly from the enzyme-treated and triturated SON tissue from three animals (one female and two male rats) at three different times. Following total RNA extraction and reverse-transcription from these single cells, PCR for VP and OT was performed to determine whether the collected cells were MNCs. Either or both OT and VP mRNA were detected in all dissociated cells

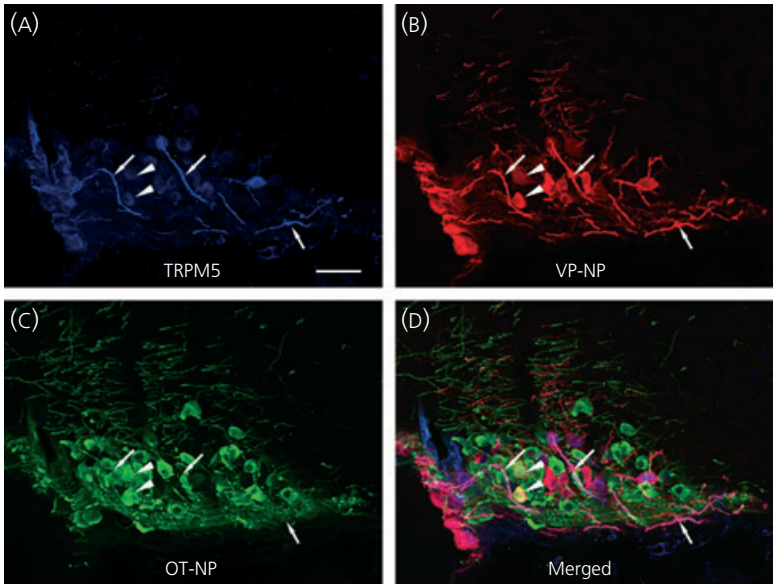

Fig. 5. Confocal triple immunofluorescence of TRPM5, vasopressin (VP)-neurophysin (NP) and oxytocin (OT)-NP in the supraoptic nucleus (SON). (A) Confocal photomicrographs of TRPM5 immunoreactivity labelled with Alexa Fluor 647-conjugated secondary antibody in the SON. The most intense TRPM5 immunoreactivity was observed in the thick dendritic processes within the SON (arrows). Less intense but prominent TRPM5 immunoreactivity was also observed in the cell bodies. (B) VP-NP immunoreactivity labelled with Alexa Fluor 594-conjugated secondary antibody in the same optical section as in (A). (C) OT-NP immunoreactivity labelled with Alexa Fluor 488-conjugated secondary antibody in the same 2-μm optical section as in (A) and (B). (D) Merged image of (A), (B) and (C). TRPM5 immunoreactivities were co-localised well with those of VP-NP, and not OT-NP. These co-localisations are indicated by purple colour produced by overlap of the Alexa Fluor 647 and 594 labelled elements. Note there is no co-localisation of TRPM5 and OT-NP immunoreactivity either in the processes or cell bodies, except in rare cases where co-localisation of VP-NP and OT-NP immunoreactivites occured. These cases are indicated by the yellow colour and arrowheads. Scale bar = 50 μm.

collected. It must be noted that our data and data obtained from previous studies (21–23) clearly show that, in most neurones, there was co-localisation of OT mRNA and VP mRNA. However, in most cases, cells were predominately positive for one or the other mRNA. However, this RT-PCR assay is sensitive, but not quantitative, so that the absolute levels of OT and VP are unknown. The cDNA from each MNC was amplified by PCR for TRPM4 and TRPM5. Amplified products of expected size for TRPM4 were obtained from cDNA libraries derived from eight out of nine MNCs from a female rat, and six out of 12 MNCs, and six out of seven (Fig. 7C), from two male rats, respectively. Unfortunately, the reaction was not robust in TRPM5 PCR and reliably detectable amounts of amplified product were not obtained at single-cell RT-PCR.

Discussion

The major finding of the present study is that TRPM5 was localised primarily in the soma and dendrites of VP neurones. Approximately one-third of the MNCs are known to reside in the accessory nuclei outside the SON and PVN (24). Both TRPM4 and TRPM5 immunoreactivities were observed in the nucleus circularis and neurones within the medial forebrain bundle in the lateral hypothalamus. These accessory nuclei are known to contain both VP and OT MNCs. However, the TRPM5 immunoreactivities were not observed in other MNCs, such as those in the anterior commissural nucleus (aka as rostral PVN) and the magnocellular periventricular nucleus, which are two nuclei almost exclusively composed of OT neurones (25, 26). This anatomical finding further supports the hypothesis that TRPM5 is associated more with VP than OT neurones. In addition, although TRPM5 mRNA was not detected by single-cell RT-PCR, it was found in cDNA libraries derived from the punched SON tissues. It appears likely that that absence of single-cell detection probably reflects a difference either in the efficiency of the probe and/or reduced expression of TRPM5. An alternative explanation is that the dissociation process in single-cell RT-PCR severed dendrites and some TRPM5 mRNA was lost with the dendrites. It is well documented that protein synthetic machinery are located not only in cell body, but also in dendrites (27), and the intense TRPM5 immunoreactivity observed in thick dendrites could indicate significant local synthesis. Regardless, these findings make TRPM5 a serious candidate for the channel type mediating the generation of fDAPs that are more specifically expressed by VP neurones.

TRPM4 was described in wide variety of mammalian tissues, kidney, heart (12, 13, 19), cerebral arteries (28, 29), microglia cells of the central nervous system (30), pancreatic β-cells (31, 32), pancreatic α-cells (33) and immune cells (34, 35). The distribution of TRPM4 in kidney, heart and cerebral arteries indicates that this channel may play a role in the cardiovascular system. In the heart, the high expression of TRPM4 was demonstrated in mouse-sinoatrial node cells (36). Indeed, the expression of TRPM4 was present to a greater degree in the atrial myocardium than in the ventricular myocardium (37). It was therefore speculated that TRPM4 is a can-

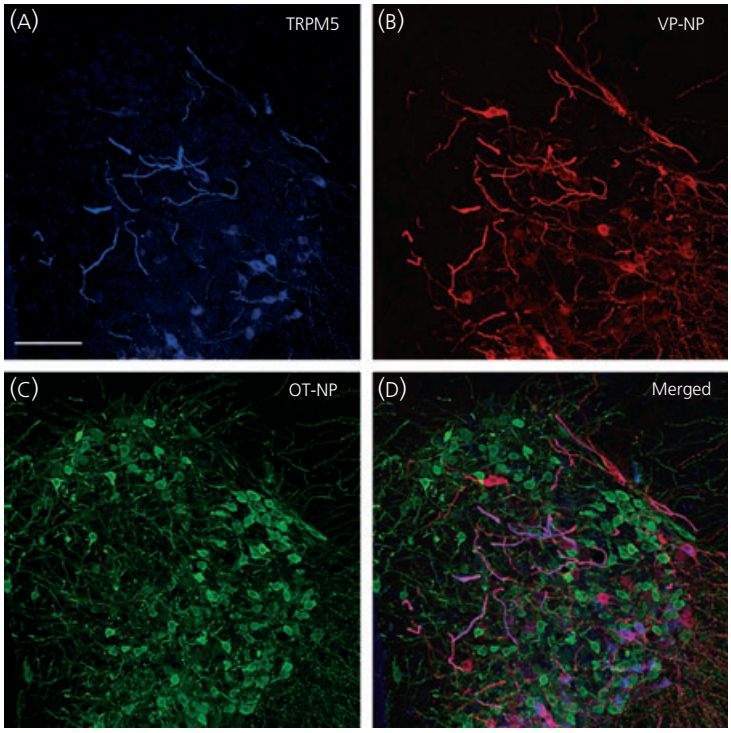

Fig. 6. Confocal triple immunofluorescence of TRPM5, vasopressin (VP)-neurophysin (NP) and oxytocin (OT)-NP in the paraventricular nucleus (PVN). (A) Confocal photomicrographs of TRPM5 immunoreactivity labelled with Alexa Fluor 647-conjugated secondary antibody in the PVN. As in the supraoptic nucleus, the most intense TRPM5 immunoreactivity was observed in the thick dendritic processes in the PVN. (B, C) VP-NP and OT-NP immunoreactivities labelled with Alexa Fluor 594 and 488-conjugated secondary antibodies, respectively, in the same optical section as in (A). (D) Merged image of (A), (B) and (C). TRPM5 immunoreactivity is co-localised well with that of VP-NP, and not OT-NP. These co-localisations are indicated by a purple colour produced by overlap of the Alexa Fluor 647 and 594 labelled elements. Note there is no co-localisation of TRPM5 and OT-NP immunoreactivity either in the processes or cell bodies because the OT-NP immunoreactivity represented by the green colour remains green in the merged image. Scale bar = 50 μm.

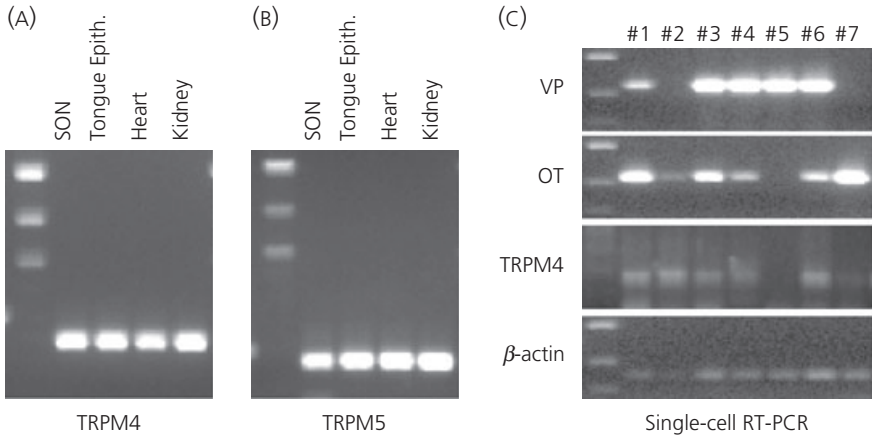

Fig. 7. (A, B) Reverse transcriptase-polymerase chain reaction (RT-PCR) detection of TRPM4 and TRPM5 in the supraoptic nucleus (SON). The mRNA coding for TRPM4 and TRPM5 is expressed in the SON. Total RNA was extracted from the SON tissue carefully punched out from brain slices, and reverse transcribed. Amplified products of the expected sizes were obtained for TRPM4 (267 bp), TRPM5 (379 bp). Rat kidney, heart and tongue epithelial tissues known to express TRPM4 and/or TRPM5 served as positive controls. Negative control reactions were performed without reverse transcriptase and amplified nothing. (C) Single-cell RT-PCR detection of TRPM4 in the magnocellular cells (MNCs). Individually dissociated MNCs were collected singly from the SON tissue. Following total RNA extraction and RT from these single cells, PCR for vasoporessin (VP) and oxytocin (OT) were performed to verify that the collected cells were MNCs. Either or both OT and VP mRNA were detected in all dissociated cell collected. Because this RT-PCR assay is sensitive, both OT and VP mRNA were detected in the most of MNCs. Because this technique is not quantitative, the cell types of the MNCs should not be determined based on the intensity of the bands on the gel. Nevertheless, this assay demonstrated that these cells are indeed MNCs. The cDNA from each MNC were amplified by PCR for TRPM4 and TRPM5. Amplified products of expected size for TRPM4 were obtained from five out of seven cDNA libraries derived from those single MNCs. The housekeeping gene β-actin was expressed in all MNCs collected, confirming that intact mRNA was isolated from each of these cells.

didate for the ion channels supporting the delayed after-depolarisation observed under conditions of Ca^{2+} overload, which might cause irregular electrical activity. Interestingly, increased TRPM4 expression in cardiac hypertrophy was observed in freshly-isolated ventricular myocytes from spontaneously hypertensive rats (38).

In the cerebral artery myocytes, TRPM4 mRNA was detected in both whole cerebral arteries and in isolated vascular smooth muscle cells (28, 29). Pressure-induced smooth muscle cell depolarisation and its resulting pressure-induced myogenic tone were attenuated in isolated cerebral arteries treated with TRPM4 antisense oligodeoxynucleotides to down-regulate channel subunits expression (28). Moreover, *in vivo* suppression of TRPM4 decreases cerebral artery myogenic constrictions and impairs autoregulation (39). Thus, these findings implicate TRPM4 channels and myogenic constriction as major contributors to cerebral blood flow regulation.

Several studies also demonstrate the functional significance of TRPM4 in noncardiovascular-related cell types. In the rat β-cell line INS-1, inhibition of TRPM4 decreases insulin secretion in response to glucose and VP stimulation (31, 32). Thus, TRPM4 dysfunction was suggested to be an important factor in the aetiology of type 2 diabetes. In T lymphocytes, TRPM4 mediates the depolarisation that plays an essential role in shaping the pattern of intracellular Ca^{++} oscillations leading to cytokine secretion (34, 35).

TRPM5 mRNA is also detected in a variety of other tissues, including taste buds, stomach, small intestine, liver, lungs, testis and brain (11, 20). Endogenous TRPM5 expression could also be detected in many cell lines, including the neuroneal cells (Cath.a), Burkitt lymphoma cells (Ramos), muring B-lymphoma cells (A20), epithelial cervical cancer-derived cells (HeLa) and murine pancreatic beta cells (MIN6) (40). However, the functional significance of TRPM5 has been most extensively studied in taste receptor cells. TRPM5 is linked to the activation of G-protein-coupled taste receptors (41–43) and is assumed to generate the depolarising receptor potential needed for the transduction of sweet, bitter and umami tastes (43–45), as well as other chemosensory stimuli (46, 47). Indeed, $TRPM5^{-/-}$ (knockout) mice have minimal ability to detect physiologically relevant concentrations of bitter or sweet substances (43, 44).

Both TRPM4 and TRPM5 mRNAs were detected in the preBötzinger complex in the brain stem (48, 49), which is essential for generation of the respiratory rhythm. It is speculated that these channels in the preBötzinger inspiratory neurones mediate the generation of a transient depolarisation, dubbed the inspiratory drive potential.

Another intriguing finding of the present study is that most intense TRPM5 immunoreactivity was located in thick dendritic processes of VP neurones, whereas immunoreactivity to TRPM4 was confined to the cell body. If the fDAP is mediated by TRPM5, this observation implies that the fDAP originates in dendrites as well as in cell bodies, where weaker but still prominent TRPM5 immunoreactivity was observed. Phasic bursting activity and DAPs are commonly observed in brain slice or hypothalamic explant preparations (50–53); however, only a small proportion (16%) of MNCs displayed spontaneous bursting activity or DAP in isolated cells (54). Therefore, the diminished expression of DAP in the isolated MNCs could be attributed to truncated dendrites during cell dissociation process.

In conclusion, the relatively selective distribution of TRPM5 immunoreactivity in VP neurones implicates the involvement of these channels in the generation of the specific fDAP (or perhaps, some other CAN-mediated potentials) and, subsequently, in the generation of the specific phasic bursting firing pattern observed in VP neurones necessary for appropriate release of VP. Future studies in knockout animals for TRPM4 and TRPM5 will prove useful for testing this hypothesis, as would other manipulations of the expression of these channels. The preferred localisation of TRPM5 to dendrites may suggest an important role of these processes in generating the fDAP.

Acknowledgements

We thank Drs. J.T. Caprio, E.L. Gleeason, and H. Cheng for reading earlier versions of this manuscript and Dr. M.A. Knepper for expert help in designing antigen.

Received 7 July 2011,
revised 2 August 2011,
accepted 13 August 2011

References

1 Brimble MJ, Dyball RE. Characterization of the responses of oxytocin- and vasopressin- secreting neurones in the supraoptic nucleus to osmotic stimulation. *J Physiol* 1977; **271**: 253–271.
2 Harris MC, Dreifuss J-J, Legros J-J. Excitation of phasically firing supraoptic neurones during vasopressin release. *Nature* 1975; **258**: 80–82.
3 Shen E, Dun SL, Ren C, Bennett-Clarke C, Dun NJ. Hypotension preferentially induces c-fos immunoreactivity in supraoptic vasopressin neurons. *Brain Res* 1992; **593**: 136–139.
4 Cazalis M, Dayanithi G, Nordmann JJ. The role of patterned burst and interburst interval on the excitation-coupling mechanism in the isolated rat neural lobe. *J Physiol* 1985; **369**: 45–60.
5 Poulain DA, Wakerley JB. Electrophysiology of hypothalamic magnocellular neurones secreting oxytocin and vasopressin. *Neuroscience* 1982; **7**: 773–808.
6 Dutton A, Dyball REJ. Phasic firing enhances vasopressin release from the rat neurohypophysis. *J Physiol* 1979; **290**: 433–440.
7 Andrew RD, Dudek FE. Analysis of intracellularly recorded phasic bursting by mammalian neuroendocrine cells. *J Neurophysiol* 1984; **51**: 552–566.
8 Ghamari-Langroudi M, Glavinovic MI. Changes of spontaneous miniature excitatory postsynaptic currents in rat hippocampal pyramidal cells induced by aniracetam. *Pflugers Arch* 1998; **435**: 185–192.
9 Bourque CW, Randle JC, Renaud LP. Non-synaptic depolarizing potentials in rat supraoptic neurones recorded in vitro. *J Physiol* 1986; **376**: 493–505.
10 Teruyama R, Armstrong WE. Calcium-dependent fast depolarizing afterpotentials in vasopressin neurons in the rat supraoptic nucleus. *J Neurophysiol* 2007; **98**: 2612–2621.
11 Hofmann T, Chubanov V, Gudermann T, Montell C. TRPM5 is a voltage-modulated and Ca(2+)-activated monovalent selective cation channel. *Curr Biol* 2003; **13**: 1153–1158.
12 Launay P, Fleig A, Perraud AL, Scharenberg AM, Penner R, Kinet JP. TRPM4 is a Ca^{2+}-activated nonselective cation channel mediating cell membrane depolarization. *Cell* 2002; **109**: 397–407.
13 Nilius B, Prenen J, Droogmans G, Voets T, Vennekens R, Freichel M, Wissenbach U, Flockerzi V. Voltage dependence of the Ca^{2+}-activated cation channel TRPM4. *J Biol Chem* 2003; **278**: 30813–30820.

14 Nilius B, Prenen J, Janssens A, Owsianik G, Wang C, Zhu MX, Voets T. The selectivity filter of the cation channel TRPM4. *J Biol Chem* 2005; **280**: 22899–22906.

15 Ullrich ND, Voets T, Prenen J, Vennekens R, Talavera K, Droogmans G, Nilius B. Comparison of functional properties of the Ca^{2+}-activated cation channels TRPM4 and TRPM5 from mice. *Cell Calcium* 2005; **37**: 267–278.

16 Ben-Barak Y, Russell JT, Whitnall MH, Ozato K, Gainer H. Neurophysin in the hypothalamo-neurohypophysial system. I. Production and characterization of monoclonal antibodies. *J Neurosci* 1985; **5**: 81–97.

17 Kunert-Keil C, Bisping F, Kruger J, Brinkmeier H. Tissue-specific expression of TRP channel genes in the mouse and its variation in three different mouse strains. *BMC Genomics* 2006; **7**: 159.

18 Enklaar T, Esswein M, Oswald M, Hilbert K, Winterpacht A, Higgins M, Zabel B, Prawitt D. Mtr1, a novel biallelically expressed gene in the center of the mouse distal chromosome 7 imprinting cluster, is a member of the Trp gene family. *Genomics* 2000; **67**: 179–187.

19 Guinamard R, Chatelier A, Demion M, Potreau D, Patri S, Rahmati M, Bois P. Functional characterization of a Ca(2+)-activated non-selective cation channel in human atrial cardiomyocytes. *J Physiol* 2004; **558** (Pt 1): 75–83.

20 Perez CA, Huang L, Rong M, Kozak JA, Preuss AK, Zhang H, Max M, Margolskee RF. A transient receptor potential channel expressed in taste receptor cells. *Nat Neurosci* 2002; **5**: 1169–1176.

21 Yamashita M, Glasgow E, Zhang BJ, Kusano K, Gainer H. Identification of cell-specific messenger ribonucleic acids in oxytocinergic and vasopressinergic magnocellular neurons in rat supraoptic nucleus by single-cell differential hybridization. *Endocrinology* 2002; **143**: 4464–4476.

22 Glasgow E, Kusano K, Chin H, Mezey E, Young WS III, Gainer H. Single cell reverse transcription-polymerase chain reaction analysis of rat supraoptic magnocellular neurons: neuropeptide phenotypes and high voltage-gated calcium channel subtypes. *Endocrinology* 1999; **140**: 5391–5401.

23 Xi D, Kusano K, Gainer H. Quantitative analysis of oxytocin and vasopressin messenger ribonucleic acids in single magnocellular neurons isolated from supraoptic nucleus of rat hypothalamus. *Endocrinology* 1999; **140**: 4677–4682.

24 Rhodes CH, Morrell JI, Pfaff DW. Immunohistochemical analysis of magnocellular elements in rat hypothalamus: distribution and numbers of cells containing neurophysin, oxytocin, and vasopressin. *J Comp Neurol* 1981; **198**: 45–64.

25 Swanson LW, Kuypers HG. The paraventricular nucleus of the hypothalamus: cytoarchitectonic subdivisions and organization of projections to the pituitary, dorsal vagal complex, and spinal cord as demonstrated by retrograde fluorescence double-labeling methods. *J Comp Neurol* 1980; **194**: 555–570.

26 Swanson LW, Sawchenko PE, Lind RW. Regulation of multiple peptides in CRF parvocellular neurosecretory neurons: implications for the stress response. *Prog Brain Res* 1986; **681**: 69–90.

27 Schuman EM, Dynes JL, Steward O. Synaptic regulation of translation of dendritic mRNAs. *J Neurosci* 2006; **26**: 7143–7146.

28 Earley S, Waldron BJ, Brayden JE. Critical role for transient receptor potential channel TRPM4 in myogenic constriction of cerebral arteries. *Circ Res* 2004; **95**: 922–929.

29 Morita H, Honda A, Inoue R, Ito Y, Abe K, Nelson MT, Brayden JE. Membrane stretch-induced activation of a TRPM4-like nonselective cation channel in cerebral artery myocytes. *J Pharmacol Sci* 2007; **103**: 417–426.

30 Beck A, Penner R, Fleig A. Lipopolysaccharide-induced down-regulation of Ca^{2+} release-activated Ca^{2+} currents (I CRAC) but not Ca^{2+}-activated TRPM4-like currents (I CAN) in cultured mouse microglial cells. *J Physiol* 2008; **586**: 427–439.

31 Cheng H, Beck A, Launay P, Gross SA, Stokes AJ, Kinet JP, Fleig A, Penner R. TRPM4 controls insulin secretion in pancreatic beta-cells. *Cell Calcium* 2007; **41**: 51–61.

32 Marigo V, Courville K, Hsu WH, Feng JM, Cheng H. TRPM4 impacts on Ca^{2+} signals during agonist-induced insulin secretion in pancreatic beta-cells. *Mol Cell Endocrinol* 2009; **299**: 194–203.

33 Nelson PL, Zolochevska O, Figueiredo ML, Soliman A, Hsu WH, Feng JM, Zhang H, Cheng H. Regulation of Ca(2+)-entry in pancreatic alpha-cell line by transient receptor potential melastatin 4 plays a vital role in glucagon release. *Mol Cell Endocrinol* 2011; **335**: 126–134.

34 Launay P, Cheng H, Srivatsan S, Penner R, Fleig A, Kinet JP. TRPM4 regulates calcium oscillations after T cell activation. *Science* 2004; **306**: 1374–1377.

35 Vennekens R, Olausson J, Meissner M, Bloch W, Mathar I, Philipp SE, Schmitz F, Weissgerber P, Nilius B, Flockerzi V, Freichel M. Increased IgE-dependent mast cell activation and anaphylactic responses in mice lacking the calcium-activated nonselective cation channel TRPM4. *Nat Immunol* 2007; **8**: 312–320.

36 Demion M, Bois P, Launay P, Guinamard R. TRPM4, a Ca^{2+}-activated nonselective cation channel in mouse sino-atrial node cells. *Cardiovasc Res* 2007; **73**: 531–538.

37 Nilius B, Vennekens R. From cardiac cation channels to the molecular dissection of the transient receptor potential channel TRPM4. *Pflugers Arch* 2006; **453**: 313–321.

38 Guinamard R, Demion M, Magaud C, Potreau D, Bois P. Functional expression of the TRPM4 cationic current in ventricular cardiomyocytes from spontaneously hypertensive rats. *Hypertension* 2006; **48**: 587–594.

39 Reading SA, Brayden JE. Central role of TRPM4 channels in cerebral blood flow regulation. *Stroke* 2007; **38**: 2322–2328.

40 Prawitt D, Monteilh-Zoller MK, Brixel L, Spangenberg C, Zabel B, Fleig A, Penner R. TRPM5 is a transient Ca^{2+}-activated cation channel responding to rapid changes in [Ca2+]i. *Proc Natl Acad Sci USA* 2003; **100**: 15166–15171.

41 Liu D, Liman ER. Intracellular Ca^{2+} and the phospholipid PIP2 regulate the taste transduction ion channel TRPM5. *Proc Natl Acad Sci USA* 2003; **100**: 15160–15165.

42 Liman ER. TRPM5 and taste transduction. *Handb Exp Pharmacol* 2007; 287–298.

43 Zhang Y, Hoon MA, Chandrashekar J, Mueller KL, Cook B, Wu D, Zuker CS, Ryba NJ. Coding of sweet, bitter, and umami tastes: different receptor cells sharing similar signaling pathways. *Cell* 2003; **112**: 293–301.

44 Damak S, Rong M, Yasumatsu K, Kokrashvili Z, Perez CA, Shigemura N, Yoshida R, Mosinger B Jr, Glendinning JI, Ninomiya Y, Margolskee RF. Trpm5 null mice respond to bitter, sweet, and umami compounds. *Chem Senses* 2006; **31**: 253–264.

45 Talavera K, Yasumatsu K, Voets T, Droogmans G, Shigemura N, Ninomiya Y, Margolskee RF, Nilius B. Heat activation of TRPM5 underlies thermal sensitivity of sweet taste. *Nature* 2005; **438**: 1022–1025.

46 Lin W, Margolskee R, Donnert G, Hell SW, Restrepo D. Olfactory neurons expressing transient receptor potential channel M5 (TRPM5) are involved in sensing semiochemicals. *Proc Natl Acad Sci USA* 2007; **104**: 2471–2476.

47 Kaske S, Krasteva G, Konig P, Kummer W, Hofmann T, Gudermann T, Chubanov V. TRPM5, a taste-signaling transient receptor potential ion-channel, is a ubiquitous signaling component in chemosensory cells. *BMC Neurosci* 2007; **8**: 49.

48 Crowder EA, Saha MS, Pace RW, Zhang H, Prestwich GD, Del Negro CA. Phosphatidylinositol 4,5-bisphosphate regulates inspiratory burst activity in the neonatal mouse preBotzinger complex. *J Physiol* 2007; **582**: 1047–1058.

49 Mironov SL, Skorova EY. Stimulation of bursting in pre-Botzinger neurons by Epac through calcium release and modulation of TRPM4 and K-ATP channels. *J Neurochem* 2011; **117**: 295–308.
50 Andrew RD. Endogenous bursting by rat supraoptic neuroendocrine cells is calcium dependent. *J Physiol* 1987; **384**: 451–465.
51 Bourque CW, Renaud LP. Activity patterns and osmosensitivity of rat supraoptic neurones in perfused hypothalamic explants. *J Physiol* 1984; **349**: 631–642.
52 Hatton GI. Phasic bursting activity of rat paraventricular neurones in the absence of synaptic transmission. *J Physiol* 1982; **327**: 273–284.
53 Teruyama R, Armstrong WE. Calcium-dependent fast depolarizing afterpotentials in vasopressin neurons in the rat supraoptic nucleus. *J Neurophysiol* 2007; **98**: 2612–2621.
54 Oliet SH, Bourque CW. Properties of supraoptic magnocellular neurones isolated from the adult rat. *J Physiol* 1992; **455**: 291–306.

